Comparative Study of State of Charge Estimation Under Different Open Circuit Voltage Test Conditions for Lithium-Ion Batteries

Gismero, Alejandro; Stroe, Daniel-Ioan; Schaltz, Erik

Published in:
IECON 2020 The 46th Annual Conference of the IEEE Industrial Electronics Society

DOI (link to publication from Publisher):
10.1109/IECON43393.2020.9254429

Publication date:
2020

Document Version
Accepted author manuscript, peer reviewed version

Comparative Study of State of Charge Estimation Under Different Open Circuit Voltage Test Conditions for Lithium-Ion Batteries

Alejandro Gismero*, Daniel-Ioan Stroe and Erik Schaltz
Department of Energy Technology, Aalborg University,
Pontoppidanstraede 101, 9220 Aalborg, Denmark;
Email: *aga@et.aau.dk, dis@et.aau.dk (D.-I.S.), esc@et.aau.dk (E.S.)

***Abstract*—**
The state of charge (SOC) is an essential indicator needed for a proper and safe operation of a battery. A large majority of methods used to estimate SOC rely on the open circuit voltage (OCV) curve. The OCV-SOC relationship is characteristic of the battery chemistry but it may also be affected by the temperature, aging or even the measurement procedure. In this work, the effect of these factors on the OCV curve is analyzed and their influence on the SOC estimation is studied. For this purpose an extended Kalman filter (EKF) has been used to compare the SOC estimation performance under different conditions. Also, the results obtained by two different methods have been compared, at two different aging states and various temperatures in the range 5-40°C.

***Index Terms*—Lithium-ion, open circuit voltage, state of charge, Kalman filter, aging, temperature**

I. Introduction

The demand for lithium batteries has experienced a strong impulse during the last decades due to the need for efficient and reliable energy storage systems. The electric vehicle acceptance is growing in recent years because of the increasing concern about the climate change crisis combined with acquisition cost reduction associated with the economy of scale of an increasingly mature technology [1], [2].

Nevertheless, the battery is still the most critical element in EV applications, due to its cost and also because of the inherent Li-ion technology hazards if operated outside the limits specified by the manufacturer. For this reason, battery management systems (BMS) are required in order to monitor and control battery state, and thus guarantee its reliability and safety [3]. The state of charge (SOC) estimation is one of the essential tasks of a BMS as it provides information about the remaining capacity of the battery which at vehicle level means the range left before having to stop and charge.

The state of charge cannot be measured directly, so it must be estimated from parameters such as the voltage or current flowing through the battery. There are different approaches to estimate the SOC, such as Coulomb counting, that calculates the remaining capacity by integrating the current [4], [5]; model based methods, which use electrochemical models [6], [7] or equivalent circuits [8] to estimate the SOC among other parameters; and data-driven methods that rely on large amounts of testing data to estimate the battery state [9].

Model based methods are widely used and provide higher accuracy as well as improved convergence compared to simpler methods based on Coulomb counting, without necessarily implying a great computational cost as in other more complex methods. These methods generally consist of a model that estimates the OCV of the battery, among other parameters. For this purpose, least Squares (LS) [10] or Kalman filter (KF) based algorithms are frequently used [11]–[14]. The SOC is finally calculated using a function that models the OCV-SOC relationship.

There are numerous reviews of the performance of these methods based on their accuracy, complexity or convergence time [15], [16]. However, the influence of the OCV-SOC curve on the performance of these methods is not analyzed in these works. The OCV-SOC relationship is influenced by factors such as temperature and battery degradation and this may affect the SOC estimation [17], [18]. In general, in BMSs for a given type of battery, a single OCV curve, usually measured at room temperature (25°C), is available. Therefore, to estimate the SOC at different temperatures may lead to a high error. Similarly, if the OCV-SOC curve has been measured at beginning of life (BOL), the error will increase as the battery ages.

Another important factor is the method used for OCV-SOC mapping, the two methods most commonly used are the incremental OCV test and the low-current OCV test, the choice may affect the SOC estimation performance.

This work deals with the differences depending on the type of OCV test as well as the influence of temperature and aging. An extended Kalman filter (EKF) is used to compare the performance of OCV curves obtained under different conditions through a discharge test based on a real driving pattern at different temperatures.

II. Methodology

In this work, 18650 Lithium Nickel Manganese Cobalt Oxide (NMC) batteries were tested with the specifications presented in Table I.

NMC-a is a fresh cell only preconditioned before the experiments while NMC-b is an aged cell which has been

This research was funded by Electric Mobility Europe Call 2016 (ERA-NET COFUND) and Innovation Fund Denmark grant number 7064-00011B.

TABLE I
CELL SPECIFICATIONS

Cell	Nominal Voltage [V]	Nominal Capacity [Ah]	Actual Capacity [Ah]
NMC-a	3.6	3.4	3.41
NMC-b	3.6	3.4	3.14

subjected to 350 full cycles following the World Harmonized Light-duty Vehicle Test Procedure (WLTP) at 25°C ambient temperature, with a consequent 8% of capacity fade after the process.

Two different methods for mapping the relationship between OCV and SOC were used, incremental and continuous charge/discharge averaging.

In the incremental OCV test, after measuring the capacity, the battery is charged and discharged in 5% SOC intervals, allowing a relaxation time of three hours between SOCs as shown in Fig. 1. The terminal voltage at the end of the pause is considered a proper approximation of the OCV. The OCV-SOC curve is obtained by averaging the values of both, charge and discharge curves.

On the contrary, in the averaging method, the battery is charged at constant rate until the upper cutoff voltage is reached and then the charge continues at constant voltage until the current is lower than 0.02C. The discharge is performed at constant current until the lower cutoff voltage is reached. Five different C-rates are used to obtain the curves, 0.2C, 0.25C, 0.5C, 0.75C and 1C as shown in Fig. 2. The OCV-SOC curve is obtained by averaging the values of both charge and discharge curves, for each considered C-rate, respectively.

The OCV-SOC relationship is measured at 5 different temperatures (5°C, 15°C, 25°C, 35°C and 40°C).

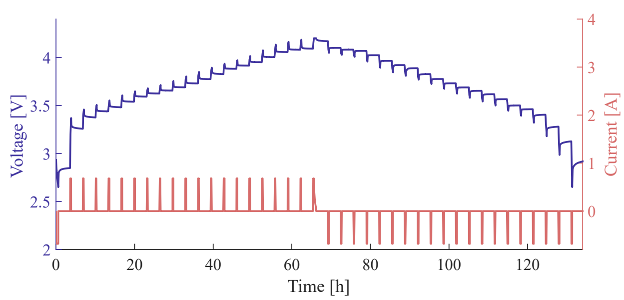

Fig. 1. Current profile and voltage response during the incremental OCV test.

A first-order RC model is adopted to estimate the dynamics of the battery during the operation as a trade-off between accuracy and complexity. The equivalent circuit used, shown in Fig. 3, consists of a resistor R_0 representing the ohmic resistance, in series with an RC branch (R_p, C_p) that reproduces the polarization characteristics of the battery. An ideal voltage source assumes the role of the OCV while V_t represents the terminal voltage; I_p is the current through R_p and I is the load current, with a positive value for charge and a negative

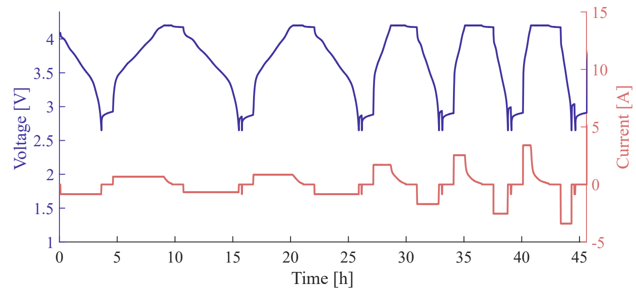

Fig. 2. Current profile and voltage response to obtain averaging OCV curves at 0.2C, 0.25C, 0.5C, 0.75C and 1C.

value for discharge. The dynamic behaviour of the battery can be described in (1).

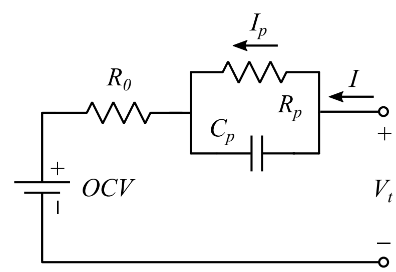

Fig. 3. First order equivalent circuit model.

$$\begin{cases} \dot{I}_p = \frac{I}{R_p C_p} - \frac{I_p}{R_p C_p} \\ V_t = OCV + R_0 I + R_p I_p \end{cases} \tag{1}$$

The equivalent circuit parameters shown above depend on variables such as temperature or SOC. Thus an EKF is used to estimate both the model parameters and the battery state defined by the OCV.

The state-space equations and the recursive computation of the filter are summarized in Table II

x_k is the system state vector at time k, u_k is the known input vector and w_k is the process noise; y_k is the output of the system and v_k is the measurement noise. w_k and v_k are independent, zero-mean, Gaussian noise processes of covariance matrices Q and R, respectively; $f()$ is the state equation and $h()$ is the output equation while A_k is the transition matrix and H_k is the measurement matrix. The detailed implementation can be found in [12]–[14].

III. OCV CURVES

This paper studies the influence of the parameters that affect the SOC-OCV curve and their impact on SOC estimation. Two different techniques for obtaining the curve have been used for this purpose, the incremental OCV test and a constant current test at different c-rates. In addition, the effect of battery aging is studied by comparing a fresh cell with one subjected to cycles. The sensitivity of the curves to temperature is also analyzed comparing the curves at 5°C, 15°C, 25°C, 35°C and 40°C.

TABLE II
SUMMARY OF THE EKF FOR ONLINE BATTERY STATE AND PARAMENTER IDENTIFICATION

State-space model:

$x_k = f(x_{k-1}, u_{k-1}) + w_k$

$y_k = h(x_k, u_k) + v_k$

Definitions:

$\hat{x}_k = [V_{oc,k} \ R_{0,k} \ R_{p,k} \ C_{p,k} \ I_{p,k}]^T$

$$A_{k-1} = \frac{\partial f(x_{k-1}, u_{k-1})}{\partial x_{k-1}}, \quad H_k = \frac{\partial h(x_k, u_{k-1})}{\partial x_k}$$

Initialization:

for $k = 0$, set:

$\hat{x}_0, P_0, Q, R$

Computation:

for $k = 1, 2, ...$, compute:

State estimate time update: $\hat{x}_k^- = f(\hat{x}_{k-1}, u_{k-1})$

Error covariance time update: $P_k^- = A_{k-1} P_{k-1} A_{k-1}^T + Q$

Kalman gain update: $L_k = P_k^- H_k^T [H_k P_k^- H_k^T + R]^{-1}$

State estimate measurement update:

$$\hat{x}_k = \hat{x}_k^- + L_k[y_k - h(\hat{x}_k^-, u_k)]$$

Error covariance measurement update: $P_k = (I - L_k H_k) P_k^-$

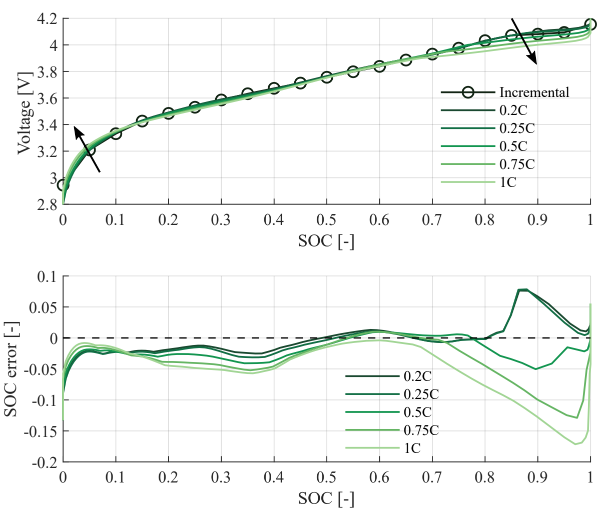

Fig. 4. OCV curves obtained through incremental test and averaging method at different C-rates.

A. OCV test influence

Fig. 4 shows the OCV curve obtained through the incremental test and the curves resulting from averaging the charge and discharge at different current levels. In the bottom graph the difference to the incremental method is shown.

Firstly, it can be observed that for these NMC cells the least steep plateau is between 85 and 95% SOC. This means that small voltage variations in this area will result in a significant deviation from the estimated SOC. In contrast, below 15% SOC the slope is higher and the error is expected to be smaller. It is also noticeable that all the curves converge around 65% SOC, so the error in that area is minimal.

Next, it should be noted that the curves obtained by averaging are similar regardless of the C-rate used, until 80% SOC is reached. From that point, the curves obtained through high currents are not capable to reflect the actual behavior of the OCV, smoothing the peak and valley that are found in that area. Compared to the incremental method, the curves obtained at 0.2C and 0.25C show a good accuracy, with an error under 3% in almost the entire SOC range until the plateau is reached where it goes up to 7%. The curve obtained at 0.5C shows an acceptable result with errors under 5% in the entire curve, while for higher C-rates the error in most part of the curve is higher.

B. Aging dependency

Fig. 5 shows the curves obtained by the incremental method both in BOL state and after 350 cycles. The error in terms of SOC between both curves is below 2% over the whole range of SOC. On the other hand, Fig. 6 shows the same curves but obtained through averaging at 0.2C. In this case the error is also small until 80% SOC is reached after which it increases up to 6%. Considering the result obtained through the incremental method, it can be deduced that the slower dynamic response due to the degradation of the battery does not allow to model the OCV correctly at that C-rate, as in the previous case with high currents.

C. Temperature sensivity

Fig. 7 shows the curves obtained at different temperatures using the incremental method and compared with that obtained at 25°C. It can be observed that the lower the temperature, the higher the OCV at low SOC levels, showing the opposite behavior at the upper end of the curve. Again, there is a convergence point of the curves around 65% SOC.

Although the greatest difference in voltage is below 20% SOC, the greatest error in terms of SOC occurs again above 80% due to the plateau in that area. The difference between the 25°C curve and the higher temperature curves remains around 1% while at low temperatures it becomes more pronounced reaching 5% for 5°C.

In the case of the curves obtained through the averaging method shown in Fig. 8, the error levels observed are similar to those obtained using the incremental method. Although the behavior is not so clear in this case, the error is around 2% in all the SOC range up to the high end of the curve where it reaches 6% for the curve obtained at 5°C.

IV. SOC ESTIMATION

To analyze the effect that the OCV curve variations have on the SOC estimation, a battery discharge test is performed. For this purpose, the battery is subjected to successive WLTP cycles alternated with 3 hours rest periods. To measure the estimation sensitivity, the EKF seen in Section II is used together with the curves obtained under different conditions of temperature and aging and through different methods, incremental test and constant current averaging.

The actual SOC reference is determined by enhanced Coulomb counting, compensating the current and temperature

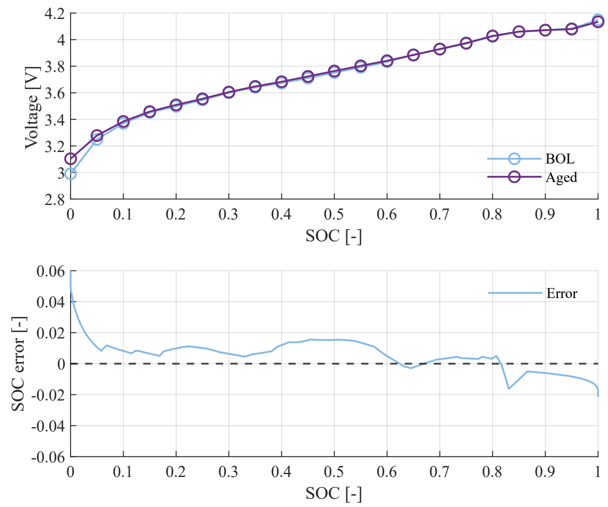

Fig. 5. OCV curves obtained by incremental test at different aging states.

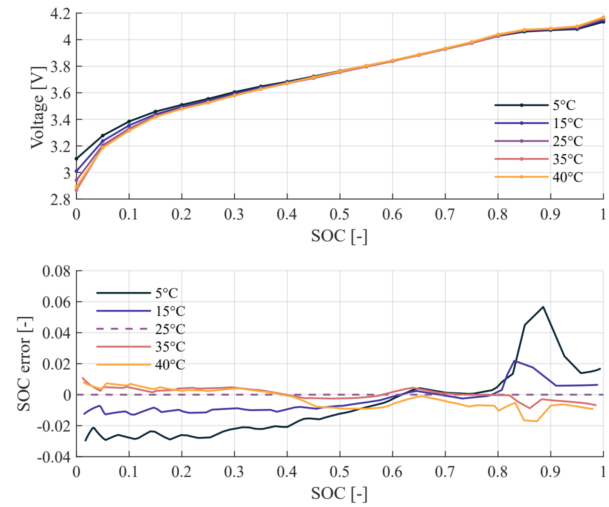

Fig. 7. OCV curves obtained by incremental test at different temperatures.

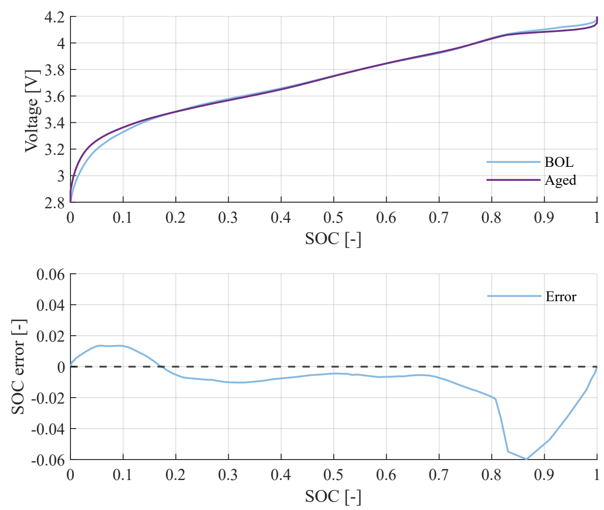

Fig. 6. OCV curves obtained by averaging test (0.2C) at different aging states.

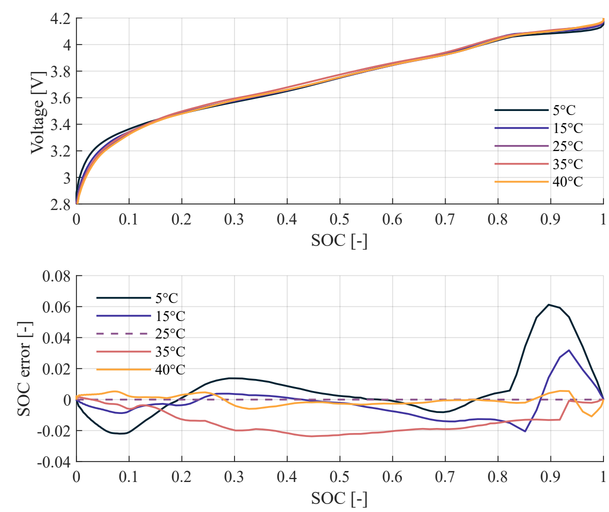

Fig. 8. OCV curves obtained by averaging test (0.2C) at different temperatures.

influence as explained in [4]. The estimation of the OCV has an initial error of 0.1 V that converges to the real value before the discharge test is started, the error analyzed corresponds only to the discharge test. Two statistical metrics are used to compare the performance, the mean absolute error (MAE) and the root mean square error (RMSE) as illustrated in (2).

$$\begin{cases} e_k = SOC_k^{EKF} - SOC_k^{actual} \\ MAE = \frac{1}{n}\sum_{k=1}^{n}|e_k| \\ RMSE = \sqrt{\frac{1}{n}\sum_{k=1}^{n}e_k^2} \end{cases} \tag{2}$$

Fig. 10 compares the SOC estimation using both the incremental and averaging methods at different C-rates, Table IV summarizes the error data. As it can be observed, the lowest error corresponds to the incremental method being below 1%. The averaging method achieves an error below 2% with C-rates of 0.2C and 0.25C, while the error is above 10% for higher C-rates. However, the results in terms of RMSE obtained by both methods at low C-rate are similar.

The effect of aging on SOC estimation and the accuracy increase that can be obtained when updating the OCV curve at the aged state are also studied. Fig. 9 shows the estimation using the BOL and aged state curves obtained with the incremental test on cell NMC-b, Table IV summarizes the error data. It is observed that the maximum error using the aged curve is below 1%, while if the curve obtained at BOL is used, this error rises above 2%.

Finally, the temperature sensitivity in the SOC estimation is analyzed. The estimation obtained when the OCV curve temperature matches the test temperature (Fig. 11) is compared with the estimation when the OCV curve is only measured at a single temperature, 25°C (Fig. 12). The error obtained in both cases is shown in Table IV. In general, it is observed that the error obtained in the second case is slightly higher, this effect being more noticeable at low SOC levels. However, the difference between both estimates is minor.

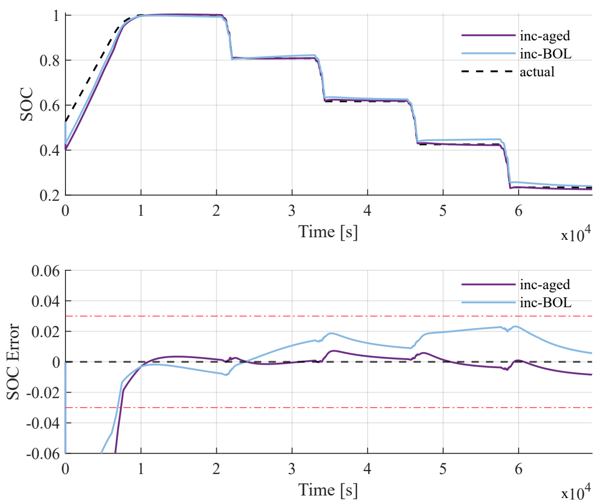

Fig. 9. SOC estimation with incremental OCV curves at different aging states.

TABLE III
SOC ERROR AT DIFFERENT AGING STATES

OCV-SOC	BOL	Aged
Max Error	0.0232	0.0084
MAE	0.0117	0.0028
RMSE	0.0134	0.0035

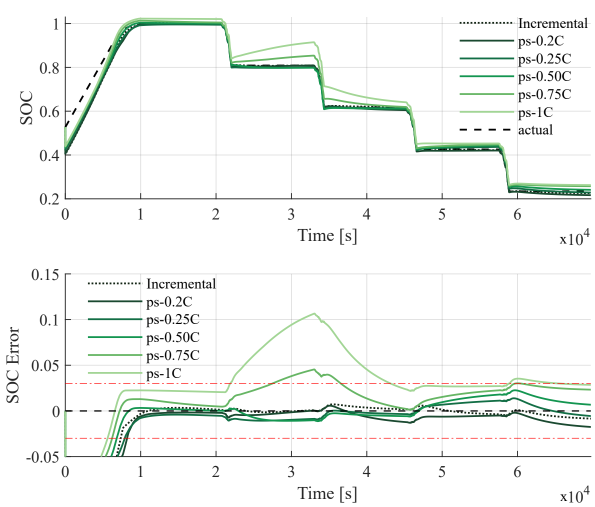

Fig. 10. SOC estimation with OCV curves obtained through different methods.

TABLE IV
SOC ERROR FOR INCREMENTAL AND AVERAGING TESTS

OCV-SOC	Inc	0.2C	0.25C	0.5C	0.75C	1C
Max Error	0.0084	0.0175	0.0149	0.0341	0.1004	0.1636
MAE	0.0028	0.0057	0.0038	0.0098	0.0289	0.0509
RMSE	0.0035	0.0071	0.0054	0.0135	0.0408	0.0696

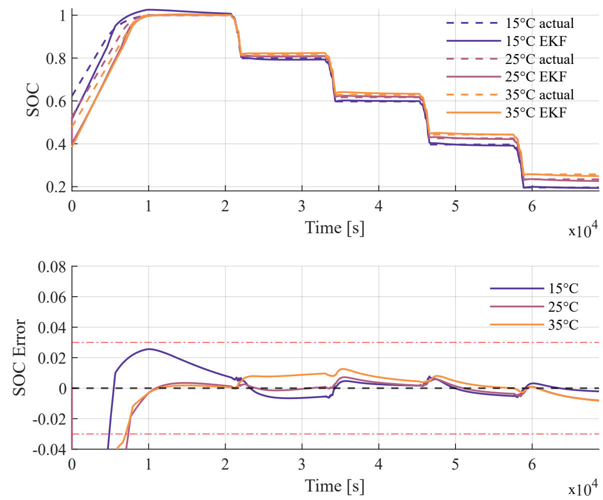

Fig. 11. SOC estimation with incremental OCV curves at different temperatures.

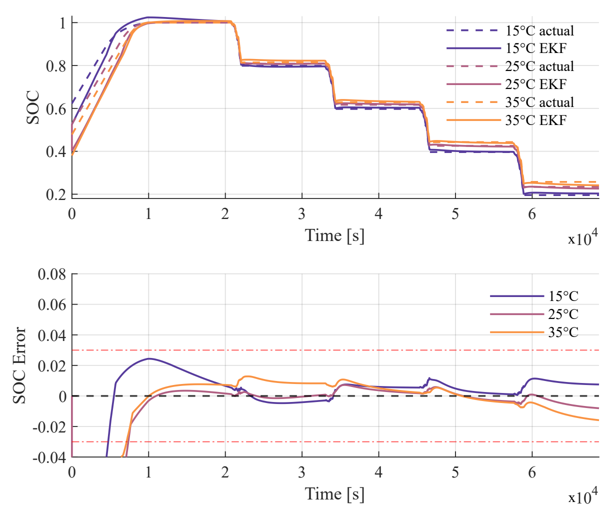

Fig. 12. SOC estimation with incremental OCV curve at 25°C.

TABLE V
SOC ERROR FOR DIFFERENT AMBIENT TEMPERATURES

Test	15°C		25°C	35°C	
OCV-SOC	15°C	25°C	25°C	35°C	25°C
Max Error	0.0255	0.0243	0.0084	0.0126	0.0163
MAE	0.0064	0.0078	0.0028	0.0050	0.0071
RMSE	0.0093	0.0097	0.0035	0.0060	0.0080

V. Conclusion

SOC estimation is one of the main tasks in battery management and although there are different methods to accomplish it, the relationship between OCV and SOC is still the basis in most of them. Therefore, it is important to consider how different factors involved in the measurement of this relationship affect the SOC estimation accuracy. In this work, two different approaches to measure the OCV curve have been studied as well as their dependence on temperature and aging. For this purpose, the SOC estimation performance has been analyzed by using an EKF, which includes the OCV among its state parameters. Thus, different OCV-SOC curves obtained under different conditions were compared. The main conclusions extracted from the results are listed below:

- The curves obtained through the incremental test show a better performance compared to those using constant current averaging, although for low current levels up to 0.25C, the result obtained are very similar for both and the error remains below 2%. Higher currents do not correctly model the behavior of the OCV and therefore should not be used.
- The aging of the cells produces slight changes in their OCV curve that affect the SOC estimation. With the cells used, after 350 cycles and 7% of capacity fading, there is twice the error, although it remains below 3%. This variation could be considerably larger at higher levels of degradation. When the curves obtained by the incremental and the averaging tests are compared, it can be concluded that, due to the aging effect on the dynamic behavior of the cell, the test conditions used to measure the OCV at BOL may not be suitable for an aged cell.
- Regarding temperature, although this is the parameter that a priory has the greatest effect on the curves, it is mainly concentrated at the lower end, where the slope is greater and, therefore, the final effect on the SOC estimation is reduced. However due to the limitations of this experiment, this could be different for other chemistries or temperatures outside the studied range.

Acknowledgment

This work has been a part of the transnational eVolution2Grid (V2G) project, supported by the Electric Mobility Europe (EMEurope) programme and Innovation Fund Denmark (Danish participants). The authors gratefully acknowledge the financial support necessary for carrying out this work.

References

[1] J. Seixas, S. Simões, L. Dias, A. Kanudia, P. Fortes, and M. Gargiulo, "Assessing the cost-effectiveness of electric vehicles in european countries using integrated modeling," *Energy Policy*, vol. 80, pp. 165 – 176, 2015.

[2] M. Dijk, R. J. Orsato, and R. Kemp, "The emergence of an electric mobility trajectory," *Energy Policy*, vol. 52, pp. 135 – 145, 2013, special Section: Transition Pathways to a Low Carbon Economy.

[3] F. H. Gandoman, J. Jaguemont, S. Goutam, R. Gopalakrishnan, Y. Firouz, T. Kalogiannis, N. Omar, and J. V. Mierlo], "Concept of reliability and safety assessment of lithium-ion batteries in electric vehicles: Basics, progress, and challenges," *Applied Energy*, vol. 251, p. 113343, 2019.

[4] A. Gismero, E. Schaltz, and D.-I. Stroe, "Recursive state of charge and state of health estimation method for lithium-ion batteries based on coulomb counting and open circuit voltage," *Energies*, vol. 13, no. 7, p. 1811, Sep 2020.

[5] K. S. Ng, C.-S. Moo, Y.-P. Chen, and Y.-C. Hsieh, "Enhanced coulomb counting method for estimating state-of-charge and state-of-health of lithium-ion batteries," *Applied Energy*, vol. 86, no. 9, pp. 1506 – 1511, 2009.

[6] M. A. Rahman, S. Anwar, and A. Izadian, "Electrochemical model parameter identification of a lithium-ion battery using particle swarm optimization method," *Journal of Power Sources*, vol. 307, pp. 86 – 97, 2016.

[7] J. Marcicki, M. Canova, A. T. Conlisk, and G. Rizzoni, "Design and parametrization analysis of a reduced-order electrochemical model of graphite/lifepo4 cells for soc/soh estimation," *Journal of Power Sources*, vol. 237, pp. 310 – 324, 2013.

[8] X. Hu, S. Li, and H. Peng, "A comparative study of equivalent circuit models for li-ion batteries," *Journal of Power Sources*, vol. 198, pp. 359 – 367, 2012.

[9] E. Chemali, P. J. Kollmeyer, M. Preindl, and A. Emadi, "State-of-charge estimation of li-ion batteries using deep neural networks: A machine learning approach," *Journal of Power Sources*, vol. 400, pp. 242 – 255, 2018.

[10] X. Hu, F. Sun, Y. Zou, and H. Peng, "Online estimation of an electric vehicle lithium-ion battery using recursive least squares with forgetting," in *Proceedings of the 2011 American Control Conference*, June 2011, pp. 935–940.

[11] P. Shrivastava, T. K. Soon, M. Y. I. B. Idris, and S. Mekhilef, "Overview of model-based online state-of-charge estimation using kalman filter family for lithium-ion batteries," *Renewable and Sustainable Energy Reviews*, vol. 113, p. 109233, 2019.

[12] T. Wang, L. Pei, R. Lu, C. Zhu, and G. Wu, "Online parameter identification for lithium-ion cell in battery management system," in *2014 IEEE Vehicle Power and Propulsion Conference (VPPC)*, 2014, pp. 1–6.

[13] G. L. Plett, "Extended kalman filtering for battery management systems of lipb-based hev battery packs: Part 2. modeling and identification," *Journal of Power Sources*, vol. 134, no. 2, pp. 262 – 276, 2004.

[14] ——, *Battery Management Systems Volume II: Equivalent-Circuit Methods*. Norwood, MA, USA: Artech House, 2015.

[15] J. Meng, G. Luo, M. Ricco, M. Swierczynski, D.-I. Stroe, and R. Teodorescu, "Overview of lithium-ion battery modeling methods for state-of-charge estimation in electrical vehicles," *Applied Sciences*, vol. 8, p. 659, 04 2018.

[16] F. Yang, Y. Xing, D. Wang, and K.-L. Tsui, "A comparative study of three model-based algorithms for estimating state-of-charge of lithium-ion batteries under a new combined dynamic loading profile," *Applied Energy*, vol. 164, pp. 387 – 399, 2016.

[17] F. Zheng, Y. Xing, J. Jiang, B. Sun, J. Kim, and M. Pecht, "Influence of different open circuit voltage tests on state of charge online estimation for lithium-ion batteries," *Applied Energy*, vol. 183, pp. 513 – 525, 2016.

[18] C. Lin, Q. Yu, R. Xiong, and L. Y. Wang, "A study on the impact of open circuit voltage tests on state of charge estimation for lithium-ion batteries," *Applied Energy*, vol. 205, pp. 892 – 902, 2017.